Geophysical Prospecting, 2001, **49**, 287–299

Depth migration of shot records in heterogeneous, transversely isotropic media using optimum explicit operators

Jianfeng Zhang,[1]* D.J. Verschuur[2]† and C.P.A. Wapenaar[2]‡

[1]*Department of Engineering Mechanics, Dalian University of Technology, Dalian 116023, China, and* [2]*Delft University of Technology, Laboratory of Acoustic Imaging and Sound Control, PO Box 5046, 2600 GA Delft, The Netherlands*

Received October 1999, revision accepted October 2000

ABSTRACT

A space–frequency domain 2D depth-migration scheme is generalized for imaging in the presence of anisotropy. The anisotropy model used is that of a transversely isotropic (TI) medium with a symmetry axis that can be either vertical or tilted. In the proposed scheme the anisotropy is described in terms of Thomsen parameters; however, the scheme can accommodate a wide range of anisotropy rather than only weak anisotropy. Short spatial convolution operators are used to extrapolate the wavefields recursively in the space–frequency domain for both qP- and qSV-waves. The weighted least-squares method for designing isotropic optimum operators is extended to asymmetric optimum explicit extrapolation operators in the presence of TI media with a tilted symmetry axis. Additionally, an efficient weighted quadratic-programming design method is developed. The short spatial length of the derived operators makes it possible for the proposed scheme to handle lateral inhomogeneities. The performance of the operators, designed by combining the weighted least-squares and weighted quadratic-programming methods, is demonstrated by migration impulse responses of qP and qSV propagation modes for the weak and strong TI models with both vertical and tilted symmetry axes. Finally, a table-driven shot-record depth-migration scheme is proposed, which is illustrated for finite-difference modelled shot records in TI media.

INTRODUCTION

It has been shown by theoretical studies (Levin 1979), velocity measurements in the laboratory (Thomsen 1986) and field studies (Crampin, Chesnokov and Hipkin 1984; Ball 1995) that many sedimentary rocks exhibit anisotropy. Furthermore, these sedimentary rocks can be described, to a good approximation, as being transversely isotropic (TI) with a symmetry axis perpendicular to the bedding plane (Byun 1984). Failure to account for anisotropy in migration algorithms may lead to large positional errors (Larner and Cohen 1993) or a complete loss (Martin, Ehinger and Rasolofosaon 1992) of steeply dipping structures. Several authors have recently developed migration algorithms for anisotropic media. Sena and Toksöz (1993) and Ball (1995) extended the isotropic Kirchhoff depth-migration scheme to account for the anisotropy, using anisotropic ray tracing. Alkhalifah (1995) used a Gaussian beam algorithm for post-stack migration in 2D anisotropic media. Non-stationary phase shift and phase-shift-plus-interpolation methods have also been extended to TI media to accommodate lateral velocity variations by Ferguson and Margrave (1998) and Le Rousseau (1997), respectively. Ristow (1999) developed an implicit 2D depth-migration scheme for transversely isotropic media with a vertical symmetry axis (VTI) based on optimizing the coefficients of the finite-difference equations.

*E-mail: zjfhm@dlut.edu.cn
†E-mail: D.J.Verschuur@ctg.tudelft.nl
‡E-mail: C.P.A.Wapenaar@ctg.tudelft.nl

© 2001 European Association of Geoscientists & Engineers

Kitchenside (1993) suggested both implicit and explicit schemes of space–frequency domain migration for TI media. However, his explicit scheme uses the truncated operators that have been proved unstable for short operators (Nautiyal *et al.* 1993). Based on the modified Taylor series method (Hale 1991b) and the non-linear least-squares method (Holberg 1988) for designing isotropic optimum explicit extrapolation operators, Uzcategui (1995) presented explicit extrapolation operators for 2D VTI media and illustrated these with post-stack migrations.

Seismic wavefield extrapolation by the recursive application of an explicit, convolutional operator in the space–frequency domain has been proved a useful tool for depth migration in heterogeneous, isotropic media (Holberg 1988; Blacquière *et al.* 1989; Hale 1991b; Nautiyal *et al.* 1993; Thorbecke and Rietveld 1994). It may be more attractive for the anisotropic case because, in this situation, the ray tracing has become more complicated and time consuming. We derive stable, explicit, short spatial convolutional operators for TI media and then propose a 2D table-driven anisotropic depth-migration scheme of shot records based on explicit extrapolation operators. Here 'table-driven' indicates that the depth-extrapolation process is performed by obtaining the space-variant explicit extrapolation operators from a pre-calculated operator table (Blacquière *et al.* 1989).

Similarly to the isotropic case, the basic idea for designing the optimum explicit extrapolation operators is to find a short operator in the space–frequency domain such that its spatial Fourier transform matches the exact phase-shift extrapolation operator in the propagation region as accurately as possible and its amplitudes in the evanescent region are less than unity. Since the phase-shift extrapolation operators are not symmetric in the case of TI media with a tilted symmetry axis, we need to adapt the isotropic design method by taking into account both that the phase velocity is a function of the propagation angle and that the operator is asymmetric. We design the explicit extrapolation operators using alternative methods, i.e. weighted least-squares and weighted quadratic-programming methods. The weighted least-squares method is an extension of the work of Thorbecke (1997) for the isotropic case and the weighted quadratic-programming method is developed by introducing appropriate linear constraints on the amplitudes in the weighted least-squares method. In contrast to the non-linear optimization method (Holberg 1988; Uzcategui 1995), the weighted quadratic-programming method can obtain a stable operator at a relatively low computational cost. Here, we use exact phase-velocity functions expressed in terms of the Thomsen parameters (Tsvankin 1996). Thus the resulting scheme can accommodate a wide range of anisotropy rather than only weak anisotropy (Thomsen 1986). The only restriction we impose is that we discard those wavenumbers for which dispersion curves for up- or downgoing waves are multivalued (this may occur when the symmetry axis is tilted and the anisotropy is strong). In addition, the exact vertical wavenumber is obtained from the given values of the horizontal wavenumber using the analytical solution formulae of the quartic dispersion equations. The performance of the derived operators is demonstrated by computing migration impulse responses of qP and qSV propagation modes for weak and strong TI models with both vertical and tilted symmetry axes. In order to prevent the occurrence of 'error compensation' due to using the same extrapolation tool in both forward and inverse processes, the proposed shot-record migration scheme is tested by imaging a synthetic data set obtained with a finite-difference modelling method (Zhang and Verschuur 1999).

PHASE-SHIFT EXTRAPOLATION OPERATOR

For TI media with a symmetry axis lying in the vertical plane and making an angle of ϕ with the vertical direction, the phase velocities of qP- and qSV-waves can be expressed exactly in the Thomsen notation (Tsvankin 1996) as

$$\frac{V^2(\theta,\phi)}{V_{\mathrm{P0}}^2} = 1 + \varepsilon \sin^2(\theta-\phi) - \frac{f}{2} \pm \frac{f}{2}\sqrt{\left(1+\frac{2\varepsilon\sin^2(\theta-\phi)}{f}\right)^2 - \frac{2(\varepsilon-\delta)\sin^2 2(\theta-\phi)}{f}}, \quad (1)$$

where $f = 1 - V_{\mathrm{S0}}^2/V_{\mathrm{P0}}^2$. V_{P0} and V_{S0} are, respectively, the qP- and qSV-wave velocities in the direction parallel to the symmetry axis, ε and δ are the same as those used by Thomsen (1986) but are defined here in a coordinate system rotated through an angle ϕ. With C_{ij} denoting the elastic modulus matrix of materials, ε and δ are defined as $\varepsilon = \frac{C_{11}-C_{33}}{2C_{33}}$ and $\delta = \frac{(C_{13}+C_{44})^2-(C_{33}-C_{44})^2}{2C_{33}(C_{33}-C_{44})}$, whose values represent the strength of anisotropy. The Thomsen parameters reduce to zero in the case of isotropy. In (1), the positive sign is related to the qP-wave.

For plane waves propagating in the vertical (x,z)-plane, the phase angle θ is given by

$$\sin\theta = \frac{V(\theta,\phi)k_x}{\omega}, \quad \cos\theta = \frac{V(\theta,\phi)k_z}{\omega}. \quad (2)$$

Rewriting (1) as

$$\left[\frac{V^2(\theta,\phi)}{V_{P0}^2}-\left(1-\frac{f}{2}\right)(\sin^2\theta+\cos^2\theta)-\varepsilon\sin^2(\theta-\phi)\right]^2=\frac{f^2}{4}$$
$$\left[\left(\sin^2\theta+\cos^2\theta+\frac{2\varepsilon\sin^2(\theta-\phi)}{f}\right)^2-\frac{2(\varepsilon-\delta)\sin^2 2(\theta-\phi)}{f}\right], \tag{3}$$

and then substituting (2) into (3) yields a quartic dispersion equation of TI media (see Appendix), which is valid for arbitrary strength of the anisotropy and for both vertical and tilted symmetry axes. In contrast to the approximated solutions of k_z, such as the table-driven interpolation (Le Rousseau 1997) and the interpolating polynomial (Ferguson and Margrave 1998), we solve k_z analytically from the quartic dispersion equation (see Appendix). The four roots of the quartic dispersion equation are related to the down- and upgoing qP-waves and the down- and upgoing qSV-waves, respectively. Figure 1 shows a solution of the quartic dispersion equation for a strong TI medium with a tilted symmetry axis.

For every combination of ω/V_{P0}, ε, δ, V_{S0}/V_{P0} and ϕ, solving k_z with a positive real part (or negative imaginary part) for given values of k_x will provide the exact forward phase-shift extrapolation operator for downgoing waves as

$$\tilde{W}^+(k_x,\omega/V_{P0},\varepsilon,\delta,V_{S0}/V_{P0},\phi)=\exp(-\mathrm{i}k_z\Delta z). \tag{4}$$

Thus the inverse phase-shift extrapolation (downward continuation) operator for upgoing waves can be expressed as

$$\tilde{F}^-(k_x,\omega/V_{P0},\varepsilon,\delta,V_{S0}/V_{P0},\phi)=\frac{1}{\tilde{W}^-(k_x,\cdots)}$$
$$\approx[\tilde{W}^-(k_x,\cdots)]^*=[\tilde{W}^+(-k_x,\omega/V_{P0},\varepsilon,\delta,V_{S0}/V_{P0},\phi)]^*, \tag{5}$$

where the superscript * denotes the complex conjugate, and the superscripts + and − refer to downgoing and upgoing waves, respectively. Equation (5) is exact for propagating waves only. Note that in the space domain the relationship between the forward and inverse operators becomes

$$F^-(x,\omega/V_{P0},\varepsilon,\delta,V_{S0}/V_{P0},\phi)$$
$$\approx[W^+(x,\omega/V_{P0},\varepsilon,\delta,V_{S0}/V_{P0},\phi)]^*. \tag{6}$$

OPERATOR DESIGN

Finding a short convolutional operator by matching its spatial Fourier transform with the exact phase-shift extrapolation operator over the propagation region will make it possible to extrapolate wavefields in lateral inhomogeneous media. Of course, this explicit extrapolation operator also should decay the evanescent energy. Due to the fact that the explicit extrapolation operator is used recursively from one depth level to the next, the stability becomes a crucial problem in the design of the operator. Strictly speaking, the stability analysis of the extrapolation operators should be carried out with a singular-value decomposition when they

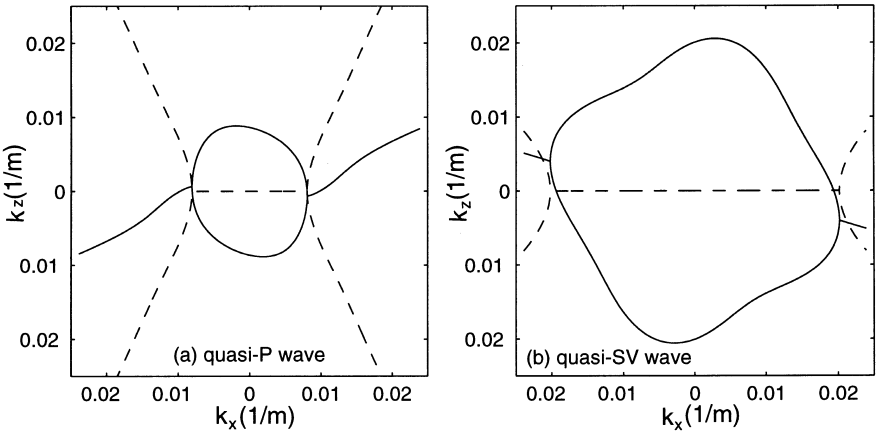

Figure 1 Dispersion relationships of qP- and qSV-waves for a TI medium with a symmetry axis making an angle of 30° with the vertical direction. The solid lines denote the real part of k_z and the dashed lines the imaginary part of k_z. The medium has a qP-wave velocity of 2700 m/s and a qSV-wave velocity of 1500 m/s in the direction parallel to the symmetry axis with the Thomsen parameters $\varepsilon = 0.2$ and $\delta = 0.5$. The frequency is 25 Hz.

are used in laterally varying media (Etgen 1994). However, from the point of view of operator design, an efficient way to achieve stability is to limit all amplitudes of the spatial Fourier transform of the operator so that they do not exceed unity, which for practical purposes means that the operator is stable for recursive applications in laterally homogeneous media. Fortunately, in most cases, the operator derived in this way can lead to a stable result when it is applied recursively in laterally inhomogeneous media (Etgen 1994). In the following, the discussions on stability refer to that of an operator used in the laterally homogeneous case, not the stability of those used in different heterogeneous media. Holberg (1988) used a non-linear constrained least-squares optimization method to derive an accurate stable explicit extrapolation operator. Hale (1991b) proposed a modified Taylor series method to guarantee that the operator would be stable. Nautiyal *et al.* (1993) designed an explicit extrapolation operator by windowing with a taper function. The methods of Hale (1991b) and Nautiyal *et al.* (1993) are both more efficient but less accurate than Holberg's (1988) method. Based on finding suitable weighting factors for components inside and outside the propagation region, the weighted least-squares method (Thorbecke and Rietveld 1994; Thorbecke 1997), although without constraints on the amplitudes, can obtain a stable explicit extrapolation operator at a very low computational cost. Due to oscillation, phase and amplitude errors partly compensate each other in waves propagating through inhomogeneous media, and thus in practice the weighted least-squares method has high accuracy.

Here we first extend the weighted least-squares method to TI media and then we propose a weighted quadratic-programming method. The latter is derived by introducing linear constraints on the amplitudes, instead of quadratic ones, in the weighted least-squares method. The linear constraints on the amplitudes used here transform the original non-linear optimization problem of operator design (Holberg 1988; Uzcategui 1995) into a quadratic-programming problem. Quadratic programming has been comprehensively studied (Fletcher 1981), and the computational cost of carrying out quadratic programming is much lower than that of non-linear optimization. This can be verified from the fact that one of the current algorithms for performing non-linear optimization transforms the non-linear optimization problem into a series of quadratic-programming problems which can be solved by many available algorithms (Fletcher 1981). Thus the weighted quadratic-programming method can derive a stable operator at a relatively low computational cost in contrast to the non-linear optimization methods.

Weighted least-squares method

If the complex vector $\mathbf{y}$ denotes the desired short convolutional operator, the discretized values of its spatial Fourier transform can be expressed as $\tilde{\mathbf{y}} = \mathbf{\Gamma y}$. Here the elements Γ_{mn} of the matrix $\mathbf{\Gamma}$ are defined as

$$\Gamma_{mn} = \exp(\mathrm{i}m\Delta k_x n\Delta x), \quad n = -N, \cdots, N, \quad m = -M, \cdots, M,$$

where $(2N+1)\Delta x$ is the length of the operator, and $M\Delta k_x$ is the maximum horizontal wavenumber. Defining the sum-of-squares error as

$$e = (\mathbf{y}^{\mathrm{H}}\mathbf{\Gamma}^{\mathrm{H}} - \tilde{\mathbf{y}}_{\mathrm{e}}^{\mathrm{H}})\mathbf{\Lambda}(\mathbf{\Gamma y} - \tilde{\mathbf{y}}_{\mathrm{e}}), \tag{7}$$

where the superscript H denotes transposition and complex conjugation, we can transform the design of the optimum operator into an unconstrained optimization problem, i.e. minimizing e. Here the complex vector $\tilde{\mathbf{y}}_{\mathrm{e}}$ contains the discretized values of the exact phase-shift extrapolation operator for $k_x = -M\Delta k_x, \cdots, M\Delta k_x$, and the weight matrix $\mathbf{\Lambda}$ is a real diagonal matrix, whose elements are determined from a weighting function described by the required range of angles of propagation and the weighting factor (Thorbecke 1997). Thus, from (7), we can solve the explicit extrapolation operator as

$$\mathbf{y} = [\mathbf{\Gamma}^{\mathrm{H}}\mathbf{\Lambda\Gamma}]^{-1}\mathbf{\Gamma}^{\mathrm{H}}\mathbf{\Lambda}\tilde{\mathbf{y}}. \tag{8}$$

Normally, a simple box function with a weight of 1.0 inside the required range of angles of propagation and a small value (e.g. 10^{-5}) outside this band will be helpful in deriving a stable operator. Figure 2 shows a wavenumber spectrum for the 39-point explicit extrapolation operator (i.e. $N = 19$). Although some of these amplitudes are greater than unity, they do not exceed 1.001, which guarantees that application of this operator for 400 steps of extrapolation in a homogeneous medium will magnify amplitudes by no more than 1.5.

Weighted quadratic-programming method

The asymmetry of the phase-shift extrapolation operator for TI media makes the design of the operators more complicated. Sometimes it is difficult for the weighted least-squares method to derive an operator having amplitudes less than a given maximum value, such as 1.001, especially in the high-frequency case. Therefore we have to introduce constraints

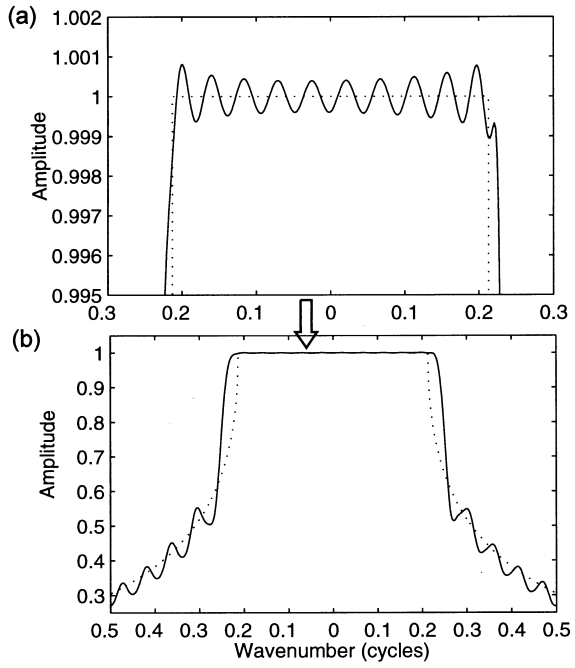

Figure 2 Wavenumber spectrum for a 39-point explicit extrapolation operator designed by the weighted least-squares method (solid lines). The required range of angles of propagation is −90° to 90°. (a) shows a detailed view of the propagation region. The dotted lines are related to the spectrum of the exact phase-shift extrapolation operator. The normalized frequency is 0.24 cycles. The operator corresponds to a TI medium with a tilted symmetry axis.

on the amplitudes in the weighted least-squares method. Conventionally, the constraints can be formulated as

$$\sqrt{a^2(k_x)+b^2(k_x)} < g, \quad k_{\min} \le k_x \le k_{\max}, \tag{9}$$

$$\sqrt{a^2(k_x)+b^2(k_x)} < 1.0, \quad k_x < k_{\min} \quad \text{and} \quad k_x > k_{\max}, \tag{10}$$

where g is the assigned maximum value of the amplitudes, $k_{\max}$ and $k_{\min}$ are, respectively, the maximum and minimum horizontal wavenumbers inside the required range of angles of propagation, $a(k_x)$ and $b(k_x)$ are, respectively, the real and imaginary parts of the spatial Fourier transform of the desired short operator at $k_x = m\Delta k_x$, and we have

$$a(m\Delta k_x) + \mathrm{i}b(m\Delta k_x) = \{\Gamma_{m(-N)}, \cdots, \Gamma_{m0}, \cdots, \Gamma_{mN}\}\mathbf{y}.$$

Note that only constraints outside the required range of angles of propagation (similar to (10)) are introduced by Holberg (1988) and Uzcategui (1995).

Unfortunately, the non-linear constraints of (9) and (10) will transform the design of the optimum operator into a non-linear constrained optimization problem. This leads to a high computational cost (Thorbecke 1997). Since the sum-of-squares error given by (7) is a quadratic function of the vector **y**, a more efficient algorithm based on quadratic programming may be obtained if the constraints of (9) and (10) can be transformed into linear constraints on the vector **y**. To achieve this, we make a distinction between the constraints inside and outside the required range of angles of propagation.

First the constraint of (9) is considered. It is known that the spatial Fourier transform of the desired short operator approaches the exact phase-shift extrapolation operator inside the required range of angles of propagation (a basic requirement for the design of the optimum operator), and we thus can approximate the constraints using the first-order Taylor series inside the required range of angles of propagation as follows:

$$\begin{aligned}\sqrt{a^2(k_x)+b^2(k_x)} \approx{}& \sqrt{\tilde{y}_{er}^2(k_x)+\tilde{y}_{ei}^2(k_x)} \\ &+ \frac{\tilde{y}_{er}(k_x)}{\sqrt{\tilde{y}_{er}^2(k_x)+\tilde{y}_{ei}^2(k_x)}}(a(k_x)-\tilde{y}_{er}(k_x)) \\ &+ \frac{\tilde{y}_{ei}(k_x)}{\sqrt{\tilde{y}_{er}^2(k_x)+\tilde{y}_{ei}^2(k_x)}}(b(k_x)-\tilde{y}_{ei}(k_x)) \\ ={}& \tilde{y}_{er}(k_x)a(k_x)+\tilde{y}_{ei}(k_x)b(k_x),\end{aligned} \tag{11}$$

where $\tilde{y}_{er}(k_x)$ and $\tilde{y}_{ei}(k_x)$ are, respectively, the real and imaginary parts of the exact phase-shift operator at $k_x = m\Delta k_x$.

Next, the second constraint of (10) is adapted. It can be seen that the highest possibility of the amplitudes of the spatial Fourier transform of the desired short operator exceeding unity outside the required range of angles of propagation occurs when its real part is greater than a positive value or its imaginary part is less than a negative value. Since the only reason for setting the constraints outside the required range of angles of propagation is to ensure that the amplitudes are less than 1.0, i.e. to decay the high-dip angle and evanescent energies, we can substitute the constraints of (10) and obtain

$$a(m\Delta k_x) < A_c \exp(-\alpha(m\Delta k_x - k_{xc})^2), \tag{12}$$

and

$$\begin{aligned}b(m\Delta k_x) &> -\beta\sqrt{1.0 - a^2(m\Delta k_x)} \\ &= -\beta\sqrt{1.0 - A_c^2 \exp(-2\alpha(m\Delta k_x - k_{xc})^2)},\end{aligned} \tag{13}$$

where k_{xc} is equivalent to either $k_{\min}$ (when $m\Delta k_x < k_{\min}$) or $k_{\max}$ (when $m\Delta k_x > k_{\max}$), $A_c = \tilde{y}_{er}(k_{xc})$, α is a parameter

selected according to the decay requirement for the amplitudes, and β is a parameter that is selected in the range $0.7 \leq \beta \leq 1.0$.

Using (11), (12) and (13), we can transform the non-linear constraints on the amplitudes into a linear one, expressed in matrix form as $\mathbf{Py} < \mathbf{q}$, for $m = -M, \cdots, M$. Thus the design of the optimum operator is reformulated, as minimizing the error function e, given by

$$e = (\mathbf{y}^{\mathrm{H}}\boldsymbol{\Gamma}^{\mathrm{H}} - \tilde{\mathbf{y}}_{\mathrm{e}}^{\mathrm{H}})\boldsymbol{\Lambda}(\boldsymbol{\Gamma}\mathbf{y} - \tilde{\mathbf{y}}_{\mathrm{e}}), \tag{14}$$

subject to the linear constraints

$$\mathbf{Py} < \mathbf{q}. \tag{15}$$

The quadratic programming of (14) and (15) can be solved efficiently with many available algorithms (Fletcher 1981).

The behaviour of the weighted quadratic-programming method is illustrated in Fig. 3, where the same weighting functions are used for both the weighted quadratic-programming and the weighted least-squares methods. It can be seen that the amplitudes of the operator derived by the weighted least-squares method (i.e. the dashed line) exceed 1.0025. This will magnify amplitudes by more than 2.7 when this operator is applied for 400 steps of extrapolation in a homogeneous medium. On the other hand, the amplitudes of the operator derived using the weighted quadratic-programming method are still less than 1.001. This is why it is sometimes necessary to use the weighted quadratic-programming method to design operators. For the results shown in Fig. 3, the computational cost of the weighted quadratic-programming method is about eight times that of the weighted least-squares method. It should also be mentioned that, in the isotropic case, the computational cost of the non-linear optimization method is over 500 times that of the weighted least-squares method (Thorbecke 1997).

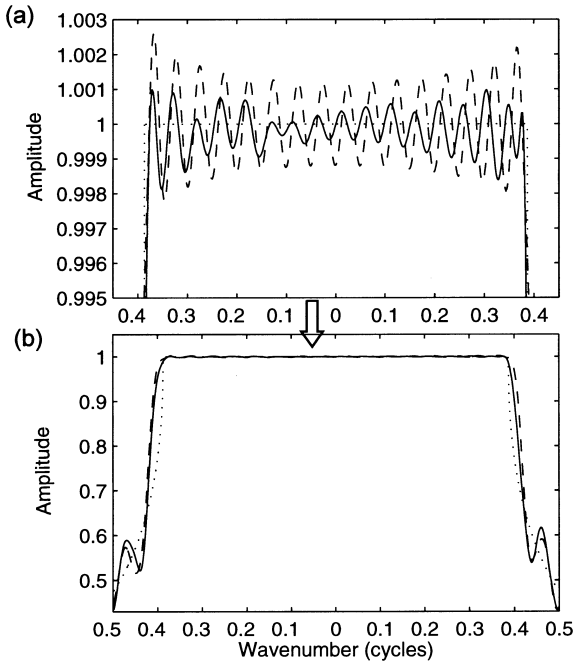

Figure 3 Comparison of the wavenumber spectra for 39-point explicit extrapolation operators designed by the weighted least-squares method (dashed line) and weighted quadratic-programming method (solid line). (a) shows a detailed view of the propagation region. The dotted line is related to the spectrum of the exact phase-shift extrapolation operator. The required range of angles of propagation is −90° to 90°. The normalized frequency is 0.43 cycles.

Here, the operators are designed by combining the weighted least-squares and weighted quadratic-programming methods, i.e. the operator is derived by first applying the weighted least-squares method and then the weighted quadratic-programming method, if the former fails to give amplitudes of less than a given value.

MIGRATION IMPULSE RESPONSE

The performance of the derived explicit extrapolation operators can best be exemplified through a study of migration impulse responses. The space–frequency domain post-stack depth-migration scheme for isotropic media (Berkhout 1982) was used here. The wavefield downward-continuation is performed in the space–frequency domain by a space-variant convolution of the data performed recursively using the operator designed for qP or qSV propagation modes as discussed in the previous section. Existing laboratory and field data indicate that the horizontal velocity of the qP-wave is usually larger than the vertical velocity, i.e. the parameter ε is predominantly positive (Thomsen 1986). Also, most measurements made for transversely isotropic formations at seismic frequencies indicate that $\varepsilon > \delta$ (Thomsen 1986; Sayers 1994; Tsvankin and Thomsen 1994). Hence, we take $\varepsilon = 0.2$ and $\delta = 0.1$ as an example of weak anisotropy and $\varepsilon = 0.4$ and $\delta = 0.2$ as an example of strong anisotropy. Figure 4 illustrates impulse responses of qP and qSV propagation modes in a VTI medium for both weak and strong anisotropy cases, where a 39-point explicit extrapolation operator (i.e. $N = 19$) designed for angles of propagation of −90° to 90° is used for inverse extrapolation of the qP or qSV wavefield. Figure 5 shows impulse responses of qP and qSV propagation modes in the same TI model as used in Fig. 4, except that the symmetry axis makes an angle of 30° with the vertical direction. Unlike the situation in Fig. 4, for which we used a symmetric operator, an asymmetric 39-point

© 2001 European Association of Geoscientists & Engineers, *Geophysical Prospecting*, **49**, 287–299

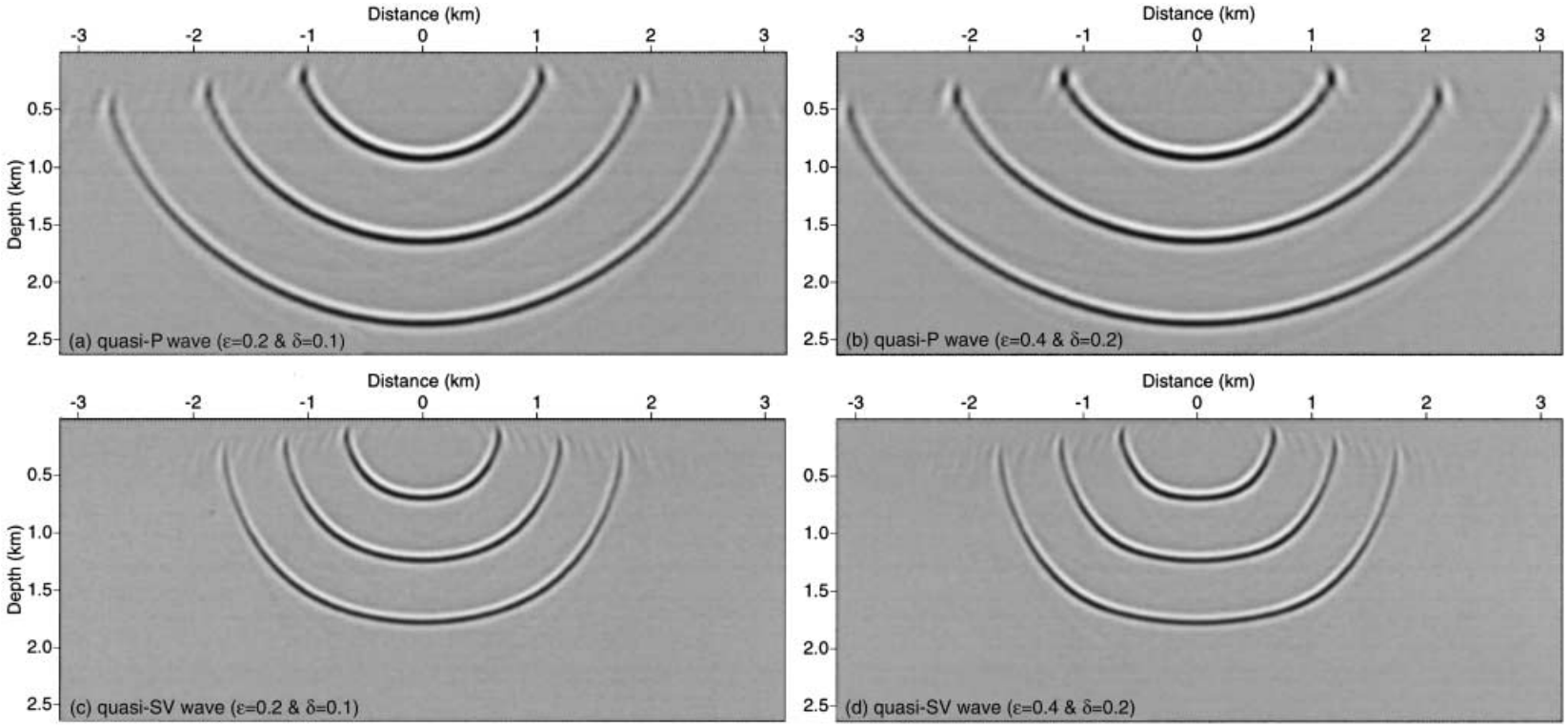

Figure 4 Migration impulse responses using symmetric 39-point explicit extrapolation operators for qP and qSV modes in a VTI medium with $V_{P0} = 2000\,\mathrm{m/s}$ and $V_{S0} = 1500\,\mathrm{m/s}$. (a) and (b) are impulse responses of the qP propagation mode, (c) and (d) of the qSV mode. The Thomsen parameters are $\varepsilon = 0.2$ and $\delta = 0.1$ for (a) and (c) and $\varepsilon = 0.4$ and $\delta = 0.2$ for (b) and (d).

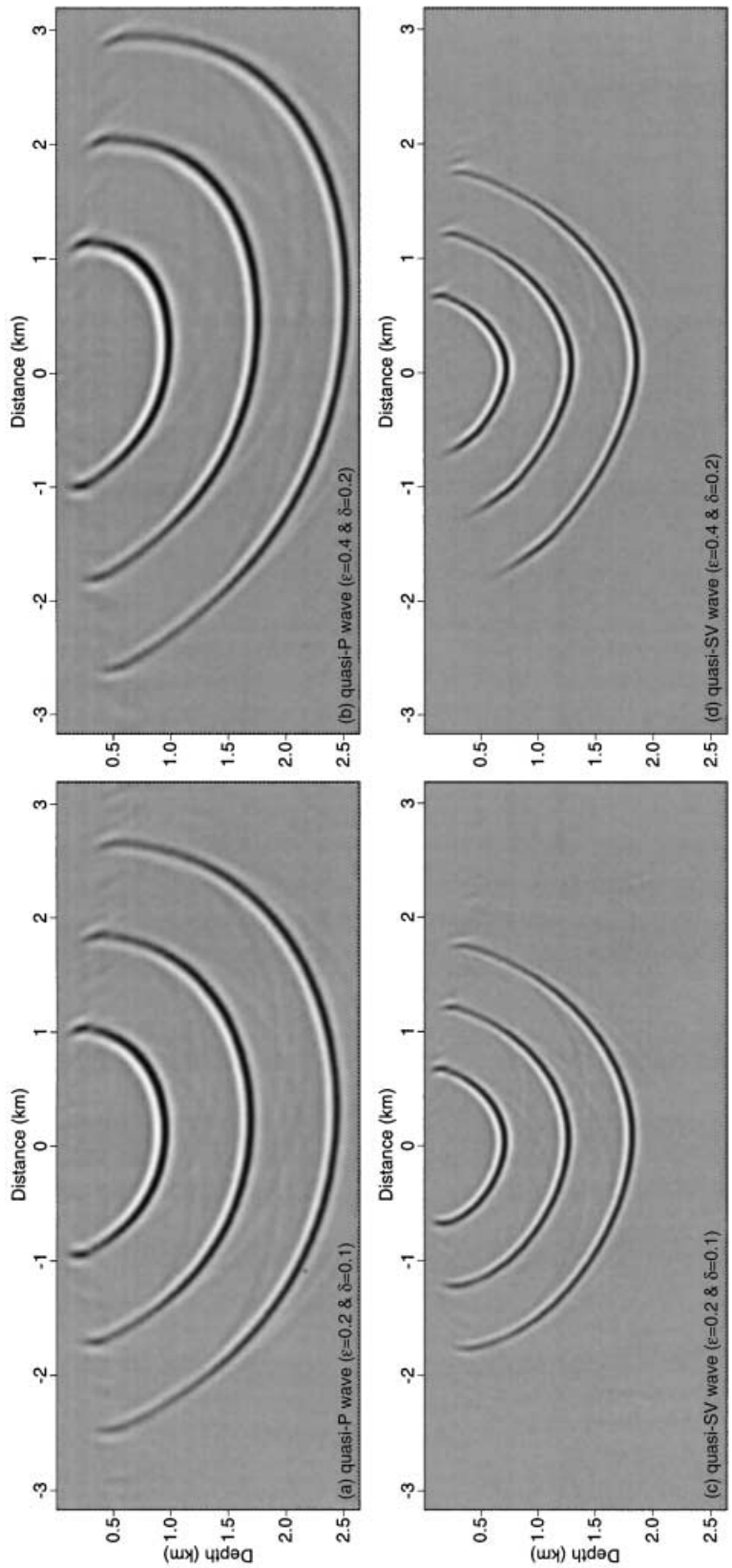

Figure 5 Migration impulse responses in a TI medium with a tilted symmetry axis. All parameters are the same as those in Fig. 4, except that the symmetry axis makes an angle of 30° with the vertical direction. Asymmetric 39-point explicit extrapolation operators are used in the migrations. (a) and (b) are impulse responses of the qP propagation mode, (c) and (d) of the qSV mode. The Thomsen parameters are $\varepsilon = 0.2$ and $\delta = 0.1$ for (a) and (c) and $\varepsilon = 0.4$ and $\delta = 0.2$ for (b) and (d).

explicit operator designed for angles of propagation of $-90°$ to 90° is now used for inverse extrapolation of the wavefield. The same zero-offset section, which contains three spatial impulses at $x = 0$ at regular time intervals, is used in all computations. Here we define the normalized frequency as $\bar{f} = f\Delta x/V_{P0}$ for the qP mode and $\bar{f} = f\Delta x/V_{S0}$ for the qSV mode. In these tests, the normalized frequency of the impulse function varies from 0 to 0.5 cycles (note that the maximum normalized frequency is 0.3 cycles in Uzcategui (1995)), and 200 recursive applications of the explicit extrapolation operator from one depth to the next, with depth steps of 13 m for the qP mode and 9.8 m for the qSV mode, are carried out. Figures 4 and 5 show that the amplitudes over a wide range of angles of propagation (approximately 80°) are well preserved. The good imaging quality in Figs 4 and 5 demonstrates the effectiveness of the design method proposed here. Although the same design methods are used, by comparing Fig. 4 with Fig. 5 it can be seen that the artefacts of the asymmetric operator are stronger than those of the symmetric one. This observation illustrates the difficulty in extending the isotropic design method to TI media.

DEPTH MIGRATION OF SHOT RECORDS

A shot record is an actual recording of a physical experiment. Since some conventional processing methods, such as normal moveout (NMO) and dip moveout (DMO), become more complicated and time consuming in the presence of anisotropy, it will be useful to perform a depth migration of individual shot records followed by common-depth-point stacking (Berkhout 1982) in anisotropic media. In our case the explicit extrapolation operators are calculated in advance and stored in a table. This table-driven extrapolation scheme is also suitable for shot-record migration because we can use the same table for wavefield extrapolation of individual shot records.

Here, the qP mode extrapolation operator table is built using the following steps: first sort a few groups of typical ε, δ, V_{S0}/V_{P0} and ϕ values from the known macro velocity model and define each group as a medium type; then assign a heterogeneous medium to each type and determine the maximum and minimum qP-wave velocities from the medium related to that type; finally, for each type calculate the optimum explicit extrapolation operators for each value of f/V_{P0} varying from $f_{min}/(V_{P0})_{max}$ to $f_{max}/(V_{P0})_{min}$ in a given interval based on the parameters, ε, δ, V_{S0}/V_{P0} and ϕ, corresponding to this type and store them in the table. The isotropic medium is classified as a special type. The effect of the parameter V_{S0}/V_{P0} on the operators is determined by the strength of anisotropy. For weak anisotropy, we can neglect the differences in V_{S0}/V_{P0} in classifying the medium type. A different medium at a different frequency can use the same operator only if they belong to the same type and their f/V_{P0} values are equal. During the depth-extrapolation process, the heterogeneous velocity model can be handled using space-variant operators obtained by picking two neighbouring operators according to the type of the local medium and the value of f/V_{P0} and then carrying out a linear interpolation.

The same space–frequency domain shot-record migration scheme as in the isotropic case (Berkhout 1982) was used here, except that the forward and inverse extrapolations of wavefields are performed using the table-driven depth-extrapolation scheme described above. With $Y_1 + iY_2$ denoting the forward extrapolation operator in the space–frequency domain, from (6) we know that the inverse extrapolation operator can be given by $Y_1 - iY_2$. Hence only the forward extrapolator operator table need be calculated and stored, even for TI media with a tilted symmetry axis. Here a synthetic example is used to illustrate the shot-record migration scheme. The subsurface velocity model is shown in Fig. 6, where the second (anisotropic) layer is a VTI medium with $V_{P0} = 2000\,\text{m/s}$, $V_{S0} = 50\,\text{m/s}$, $\varepsilon = 0.2$ and $\delta = 0.1$. The synthetic data set is generated using a finite-difference-based scheme of the two-way elastic wave equation (Zhang and Verschuur 1999), thus 'error compensations' due to using the same extrapolation tool in both forward and inverse processes are avoided. In order to produce an acoustic data set, we set the V_{S0} or V_S of all media at zero in the numerical modelling. Two typical shot gathers are shown in Figs 7(a) and 8(a). The migration results of these shot records are shown in Figs 7(b) and 8(b). In contrast, the migration results of the corresponding shot records obtained using the velocity model neglecting the anisotropy, i.e. extrapolating wavefields using isotropic extrapolation operators of $V_P = V_{P0}$, are shown in Figs 7(c) and 8(c). The common-depth-point stacked sections of 17 migrated shot records with a shot interval of 160 m and 35 migrated shot

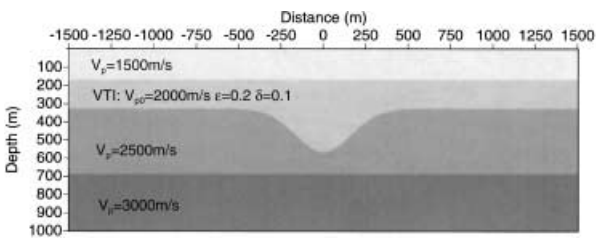

Figure 6 Subsurface velocity model with an anisotropic layer.

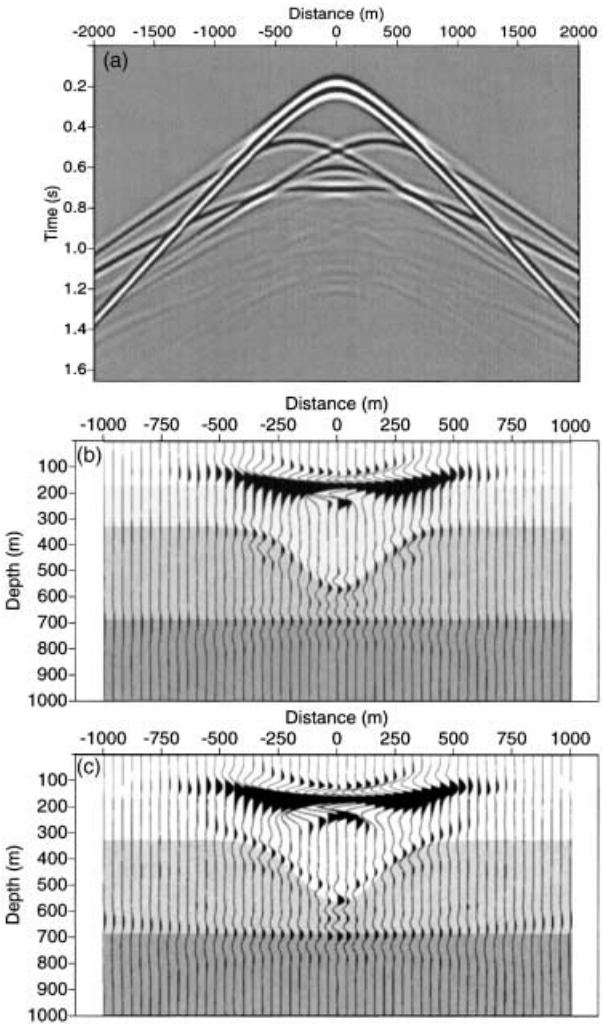

Figure 7 One shot-record result for the source positioned at $x = 0$. (a) is the shot gather obtained by the finite-difference method; (b) is the depth-migration result of this shot record using the exact velocity model; (c) is the depth-migration result using the same velocity model but neglecting the anisotropy. The backgrounds in (b) and (c) are the velocity models used.

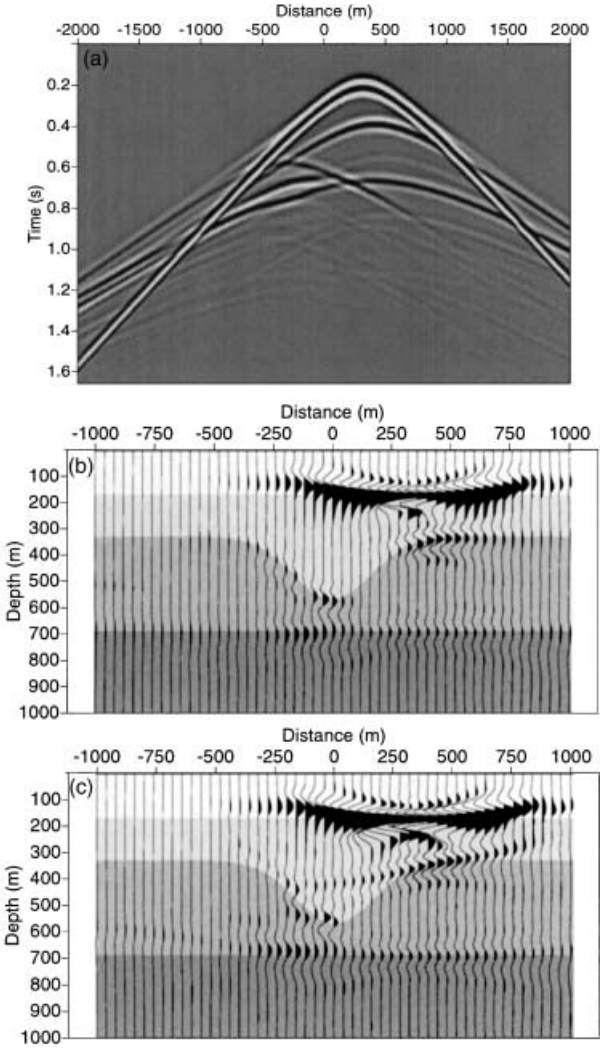

Figure 8 One shot-record result for the shot positioned at $x = 320$ m. (a) is the shot gather obtained by the finite-difference method; (b) is the depth-migration result of this shot record using the exact velocity model; (c) is the depth-migration result using the same velocity model but neglecting the anisotropy. The backgrounds in (b) and (c) are the velocity models used.

records with a shot interval of 80 m are shown in Figs 9(a) and (b), respectively. Also, a stacked section of the isotropic migration results, such as Figs 7(c) and 8(c), is shown in Fig. 10. It can be seen by comparing Figs 7(b) and 8(b) with Figs 7(c) and 8(c) that the steep structure is in the wrong position and the third flat reflector has become curved, due to neglecting anisotropy. This leads to the structures underneath the anisotropic layer becoming ambiguous in the stacked section, as observed by comparing Fig. 9(b) with Fig. 10. In Figs 7, 8, 9 and 10, the velocity model is overlain by the migrated sections. It can be seen that the peaks of the wave curves lie exactly on the interfaces when the correct velocity model is used. These observations verify that the proposed table-driven depth-extrapolation scheme for heterogeneous TI media is accurate. In all the above examples, 39-point extrapolation operators (i.e. $N = 19$) designed for angles of propagation of $-85°$ to $85°$ are used.

CONCLUSIONS

Seismic wavefield depth extrapolation using the recursive

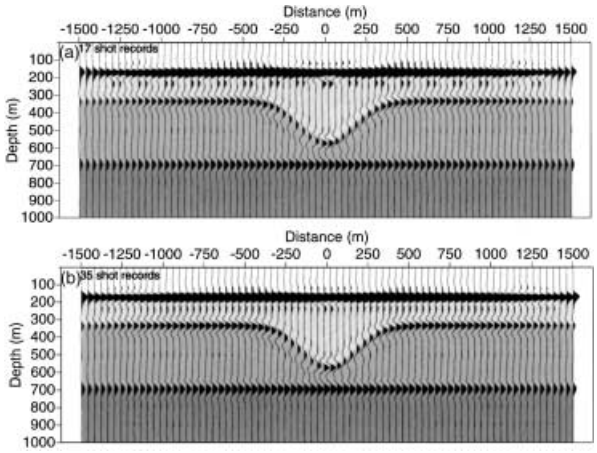

Figure 9 Prestack depth-migration result obtained using symmetric 39-point explicit extrapolation operators. The correct anisotropic velocity model is used in both examples. (a) shows the result using 17 shot records with a shot interval of 160 m; (b) shows the result for 35 shot records with a shot interval of 80 m. The background in (a) and (b) is the velocity model of Fig. 6 that is used in migrations.

application of spatial convolution operators has been extended to anisotropic media. The operator coefficients are pre-computed and made accessible in a table so that the local medium parameters and the temporal frequency are used to determine the space-variant operator at each gridpoint during the depth-extrapolation process. This table-driven depth-extrapolation scheme is especially suitable for imaging heterogeneous anisotropic media, because the added computational cost is related only to the calculation of the operator table. Moreover, the computational cost of deriving the operators for VTI media is almost the same as in the isotropic case. The methods for designing the isotropic explicit operators can be extended to anisotropic media, by bearing in mind that the desired short operator and its spatial Fourier transform are asymmetric in the presence of TI media with a tilted symmetry axis.

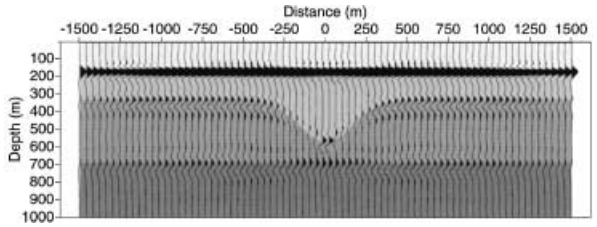

Figure 10 Effect of neglecting the anisotropy in migration. The image is the prestack depth-migration result of 35 shot records, as in Fig. 9(b), except that a velocity model neglecting anisotropy is used in the migration. Note the poor representation of the synclinal boundary and the artefacts in the third reflector.

Two design methods, weighted least squares and weighted quadratic programming, have been presented. They can design a stable explicit extrapolation operator for a low computational cost. The migration impulse responses show that the derived 39-point operators are capable of propagating waves at angles of up to 80°. Also, the artefacts produced by the 39-point operator are small. The proposed design methods are independent of the phase-shift extrapolation operator. Thus they can be used to derive the explicit extrapolation operators of arbitrary anisotropic media, including the operators for isotropic media.

All types of processing methods based on wave equations, such as post-stack depth migration and depth migration of shot records, can easily be extended to the anisotropic situation by using the table-driven depth-extrapolation scheme. The space–frequency domain depth migration of shot records is performed and is strongly recommended for imaging anisotropic structures. The numerical examples demonstrate that the proposed shot-record migration scheme can obtain an accurate subsurface structure with a sparse distribution of shot records. The examples illustrate that the structures underneath the anisotropic layer may be ambiguous when the anisotropy is neglected in the macro velocity model.

For VTI media, the 2D scheme presented here can readily be extended to accommodate full 3D processing by using McClellan transformations following Hale (1991a). For 3D depth migration in the case of TI media with an arbitrary tilted symmetry axis, we need to extend the proposed operator design method to 2D and then design asymmetric 2D explicit convolutional operators based on the 3D dispersion equation of TI media.

ACKNOWLEDGEMENTS

J.Z. thanks the National Natural Science Foundation of China and Daqing Petroleum Administration Bureau for supporting his research (under grants 49894190 and 19672016).

REFERENCES

Abramowitz M. and Stegun I.A. 1970. *Handbook of Mathematical Functions*. Dover Publications, Inc.

Alkhalifah T. 1995. Gaussian beam depth migration for anisotropic media. *Geophysics* **60**, 1474–1484.

Ball G. 1995. Estimation of anisotropy and anisotropic 3D prestack depth migration, offshore Zaire. *Geophysics* **60**, 1495–1513.

Berkhout A.J. 1982. *Seismic Migration, Imaging of Acoustic Energy*

by Wave Field Extrapolation, A: Theoretical Aspects. Elsevier Science Publishing Co.
Blacquière G., Debeye H.W.J., Wapenaar C.P.A. and Berkhout A.J. 1989. 3D table-driven migration. *Geophysical Prospecting* **37**, 925–958.
Byun B.B. 1984. Seismic parameters for transversely isotropic media. *Geophysics* **49**, 1908–1914.
Crampin S., Chesnokov E.M. and Hipkin R.A. 1984. Seismic anisotropy – the state of the art. *Geophysical Journal of the Royal Astronomical Society* **76**, 1–16.
Etgen J. 1994. Stability of explicit depth extrapolation through laterally-varying media. 64th SEG meeting, Los Angeles, USA, Expanded Abstracts, 1266–1269.
Ferguson R.J. and Margrave G.F. 1998. Depth migration in TI media by non-stationary phase shift. 68th SEG meeting, New Orleans, USA, Expanded Abstracts, 1831–1834.
Fletcher R. 1981. *Practical Method of Optimization, Volume 2, Constrained Optimization*. John Wiley & Sons, Inc.
Hale D. 1991a. 3D depth migration via McClellan transformations. *Geophysics* **56**, 1778–1785.
Hale D. 1991b. Stable explicit depth extrapolation of seismic wavefields. *Geophysics* **56**, 1770–1777.
Holberg O. 1988. Toward optimum one-way wave propagation. *Geophysical Prospecting* **36**, 99–114.
Kitchenside P.W. 1993. 2D anisotropic migration in the space–frequency domain. *Journal of Seismic Exploration* **2**, 7–22.
Larner K. and Cohen J. 1993. Migration error in transversely isotropic media with linear velocity variation in depth. *Geophysics* **58**, 1454–1467.
Le Rousseau J.H. 1997. Depth migration in heterogeneous, transversely isotropic media with the phase-shift-plus-interpolation method. 67th SEG meeting, Dallas, USA, Expanded Abstracts, 1703–1706.
Levin F.K. 1979. Seismic velocities in transversely isotropic media. *Geophysics* **44**, 918–936.
Martin D., Ehinger A. and Rasolofosaon P.N.J. 1992. Some aspects of seismic modelling and imaging in anisotropic media using laser ultrasonics. 62nd SEG meeting, New Orleans, USA, Expanded Abstracts, 1373–1376.
Nautiyal A., Gray S.H., Whitmore N.D. and Garing J.D. 1993. Stability versus accuracy for an explicit wavefield extrapolation operator. *Geophysics* **58**, 277–283.
Ristow D. 1999. Migration of transversely isotropic media using implicit finite-difference operators. *Journal of Seismic Exploration* **8**, 39–55.
Sayers C.M. 1994. The elastic anisotropy of shales. *Journal of Geophysical Research* **99**, 767–774.
Sena A.G. and Toksöz M.N. 1993. Kirchhoff migration and velocity analysis for converted and non-converted waves in anisotropic media. *Geophysics* **58**, 265–276.
Thomsen L. 1986. Weak elastic anisotropy. *Geophysics* **51**, 1954–1966.
Thorbecke J.T. 1997. *Common focus point technology*. PhD thesis, Delft University of Technology.
Thorbecke J.W. and Rietveld W.E.A. 1994. Optimum extrapolation operators – a comparison. 56th EAGE meeting, Vienna, Austria, Extended Abstracts, P105.
Tsvankin I. 1996. P-wave signatures and notation for transversely isotropic media: an overview. *Geophysics* **61**, 467–483.
Tsvankin I. and Thomsen L. 1994. Non-hyperbolic reflection moveout in anisotropic media. *Geophysics* **59**, 1290–1304.
Uzcategui O. 1995. 2D depth migration in transversely isotropic media using explicit operators. *Geophysics* **60**, 1819–1829.
Zhang J. and Verschuur D.J. 1999. Seismic modelling in anisotropic media using grid method. 61st EAGE conference, Helsinki, Finland, Extended Abstracts, 4-25.

APPENDIX A

Quartic dispersion equation and its solutions

The quartic dispersion equation of TI media is expressed as

$$k_z^4 + a_3 k_z^3 + a_2 k_z^2 + a_1 k_z + a_0 = 0, \tag{A1}$$

where

$$a_3 = [f(\varepsilon - \delta)\sin 4\phi + 2\varepsilon(1-f)\sin 2\phi]k_x/a_4$$

$$a_4 = f - 1 + 2\varepsilon(f-1)\sin^2\phi - \frac{f}{2}(\varepsilon - \delta)\sin^2 2\phi$$

$$a_2 = \left[b_2 k_x^2 + \left(\frac{\omega}{V_{P0}}\right)^2 (2 + 2\varepsilon\sin^2\phi - f)\right]/a_4$$

$$b_2 = f(\varepsilon - \delta)\sin^2 2\phi - 2(1-f)(1+\varepsilon) - 2f(\epsilon - \delta)\cos^2 2\phi$$

$$a_1 = \left[b_1 k_x^3 - 2\varepsilon\sin 2\phi\left(\frac{\omega}{V_{P0}}\right)^2 k_x\right]/a_4$$

$$b_1 = 2\varepsilon(1-f)\sin 2\phi - f(\varepsilon - \delta)\sin 4\phi$$

$$a_0 = b_0/a_4$$

$$b_0 = (2 + 2\varepsilon\cos^2\phi - f)\left(\frac{\omega}{V_{P0}}\right)^2 k_x^2 - \left(\frac{\omega}{V_{P0}}\right)^4 - \left[(1-f)(1+2\varepsilon\cos^2\phi) + \frac{f}{2}(\varepsilon - \delta)\sin^2 2\phi\right]k_x^4.$$

The analytical solutions of (A1) can be obtained by decomposing the quartic equation into two quadratic equations (Abramowitz and Stegun 1970):

$$k_z^2 + \left(a_3/2 + \sqrt{a_3^2/4 + R - a_2}\right)k_z + R/2 \pm \sqrt{R^2/4 - a_0} = 0, \tag{A2}$$

$$k_z^2 + \left(a_3/2 - \sqrt{a_3^2/4 + R - a_2}\right)k_z + R/2 \mp \sqrt{R^2/4 - a_0} = 0, \tag{A3}$$

where R is a real root of the cubic equation,

$$R^3 - a_2R^2 + (a_1a_3 - 4a_0)R - (a_1^2 + a_0a_3^2 - 4a_0a_2) = 0, \tag{A4}$$

and should give real coefficients in the quadratic equations (A2) and (A3) and satisfy

$$a_3R/2 - a_1 \mp \sqrt{(a_3^2/4 + R - a_2)(R^2/4 - a_0)} = 0. \tag{A5}$$

The three roots of (A4) are given as follows (Abramowitz and Stegun 1970):

Let

$$s_1 = [r + (q^3 + r^2)^{\frac{1}{2}}]^{\frac{1}{3}}, \quad s_2 = [r - (q^3 + r^2)^{\frac{1}{2}}]^{\frac{1}{3}},$$

where

$$q = \frac{1}{3}a_1a_3 - \frac{1}{9}a_2^2 - \frac{4}{3}a_0,$$

$$r = \frac{1}{27}a_2^3 + \frac{1}{2}a_1^2 + \frac{1}{2}a_0a_3^2 - \frac{4}{3}a_0a_2 - \frac{1}{6}a_1a_2a_3.$$

Then

$$R_1 = (s_1 + s_2) + \frac{a_2}{3}, \tag{A6}$$

$$R_2 = -\frac{1}{2}(s_1 + s_2) + \frac{a_2}{3} + \frac{i\sqrt{3}}{2}(s_1 - s_2), \tag{A7}$$

$$R_3 = -\frac{1}{2}(s_1 + s_2) + \frac{a_2}{3} - \frac{i\sqrt{3}}{2}(s_1 - s_2). \tag{A8}$$

When the negative sign makes (A5) valid, the signs in (A2) and (A3) should be, respectively, + and −, otherwise the signs should be − and +. Thus, the four roots of (A2) and (A3) are exactly the roots of the quartic equation (A1). The four roots of the quartic dispersion equation are related to the down- and upgoing qP-waves and the down- and upgoing qSV-waves, respectively.